Theor Chem Acc (2002) 107:253–265
DOI 10.1007/s00214-002-0325-2

Theoretical
Chemistry Accounts

Regular article

Theoretical study on structures and stability of HC_2P isomers

Yi-hong Ding, Ze-sheng Li, Yu-guo Tao, Xu-ri Huang, Chia-chung Sun

State Key Laboratory of Theoretical and Computational Chemistry, Institute of Theoretical Chemistry,
Jilin University, Changchun 130023, China

Received: 5 November 2000 / Accepted: 25 November 2001 / Published online: 8 April 2002

Abstract. The structures and isomerization pathways of various HC_2P isomers in both singlet and triplet states are investigated at the B3LYP/6-311G(d,p), QCISD/6-311G(d,p) (for isomers only) and single-point CCSD(T)/6-311G(d,p)//B3LYP/6-311G(d,p) levels. At the CCSD(T)/6-311G(d,p)//B3LYP/6-311G(d,p) level, the lowest-lying isomer is a linear HCCP structure ^{31} in the $^3\sum^-$ state. The second low-lying isomer has a CPC ring with exocyclic CH bonding ^{15} in a singlet state at 10.5 kcal/mol. The following third and fourth low-lying isomers are a singlet bent HCCP structure ^{11} at 20.9 kcal/mol and a bent singlet HPCC structure ^{13} at 35.8 kcal/mol, respectively. Investigation of the HC_2P potential-energy surface indicates that in addition to the experimentally known isomer ^{31}, the other isomers ^{11}, ^{13} and ^{15} also have considerable kinetic stability and may thus be observable. However, the singlet and triplet bent isomers HCPC ^{12} and ^{32} as well as the triplet bent isomer HPCC ^{33} are not only high-lying but are also kinetically unstable, in sharp contrast to the situation of the analogous HCNC and HNCC species that are both kinetically stable and that have been observed experimentally. Furthermore, the reactivity of various HC_2P isomers towards oxygen atoms is briefly discussed. The results presented here may be useful for future identification of the completely unknown yet kinetically stable HC_2P isomers ^{11}, ^{13} and ^{15} either in the laboratory or in interstellar space.

Key words: Theoretical study – Structure – Stability – Potential-energy surface – HC_2P

1 Introduction

Ever since the detection of PH_3 [1], NP [2] and CP [3] in interstellar space, considerable attention has been drawn to the possible existence of other phosphorus-containing species in space. Experimental [4] and theoretical [5] investigations have been carried out to probe their possible production mechanism in space. An important result is that phosphorus–carbon molecules, such as C_2P and HC_2P, might also exist in the molecular hot core of star-forming regions provided that oxygen atoms are not injected [6]. Stimulated by this prediction, in 1997, Ahmad et al. [7] detected the HCCP radical for the first time by microwave spectroscopy. Soon after, in 1998, Shao and Fang [8] carried out a theoretical study on the structural features of HCCP at various levels. Both studies showed that HCCP has a linear structure in a $^3\sum^-$ ground electronic state bearing both phosphoallene and phosphorene forms. To our knowledge, no theoretical calculations have been performed on the structures of other isomers of the HCCP radical or on their stability.

Chemically, HC_2P is analogous to the well-known HC_2N radical [9–13], the lowest-lying isomer, HCCN, of which has been detected in interstellar space [15] and has been the subject of numerous studies both experimentally [9–12] and theoretically [13, 14]. Nearly all the theoretical calculations showed that the triplet HCCN is a bent carbene form. Recently, the triplet bent isomers HCNC [12] and HNCC [10, 12] have also been characterized experimentally. However, the singlet CNC ring isomer with exocyclic CH bonding, which has been predicted to be the second low-lying isomer [12, 14], is still unknown even in the laboratory.

Clearly, distinct discrepancies exist between the structural features of the analogous chainlike HCCP and HCCN species [8]. Then, it is reasonable for us to wonder whether such discrepancies may also exist for other HC_2P isomers and whether their kinetic stability is high enough to allow detection. Actually, the differences between the simple molecules HCP and HCN have been well revealed, i.e., the isomer HPC is not a minimum point, whereas HNC is a kinetically stable isomer and has been detected in space. Without performing a detailed investigation on the whole potential-energy surface (PES), it still seems unlikely to be able to understand in detail the similarities and discrepancies between HC_2P and HC_2N. Therefore, a thorough the-

---

Correspondence to: Y. Ding

oretical calculation on all possible isomers of HC_2P in both the singlet and the triplet state is desirable. Such work is reported here. As will be shown, some significant discrepancies between the HC_2N and HC_2P PESs are found. Furthermore, the reactivity of HC_2P isomers towards oxygen atoms is briefly discussed.

2 Computational methods

All the calculations were carried out using the Gaussian 98 program package. The geometries of the HC_2P isomers and the interconversion transition states were fully optimized at the B3LYP/6-311G(d,p) level. Harmonic vibrational frequencies were calculated at the same level to check whether the structure obtained is a stationary point or a saddle point. To get more accurate energies, CCSD(T)/6-311G(d,p) calculations were performed at the B3LYP/6-311G(d,p) geometries. Intrinsic reaction coordinate calculations were also carried out to test whether the transition state connects the right isomers at the B3LYP/6-311G(d,p) level. For stationary isomers, further calculations were performed at the QCISD/6-311G(d,p) level to determine their structures and spectroscopic properties.

3 Results and discussions

For the tetraatomic molecule HC_2P, nearly all the possible isomeric forms were searched. Yet, only six triplet isomers (^{31}, ^{32}, ^{33}, ^{35}, ^{36} and ^{37}) and six singlet isomers (^{11}, ^{12}, ^{13}, $^33'$, ^{14} and ^{15}) are local minimum structures. A total of 17 interconversion transition states (seven in the triplet state and ten in the singlet state) were

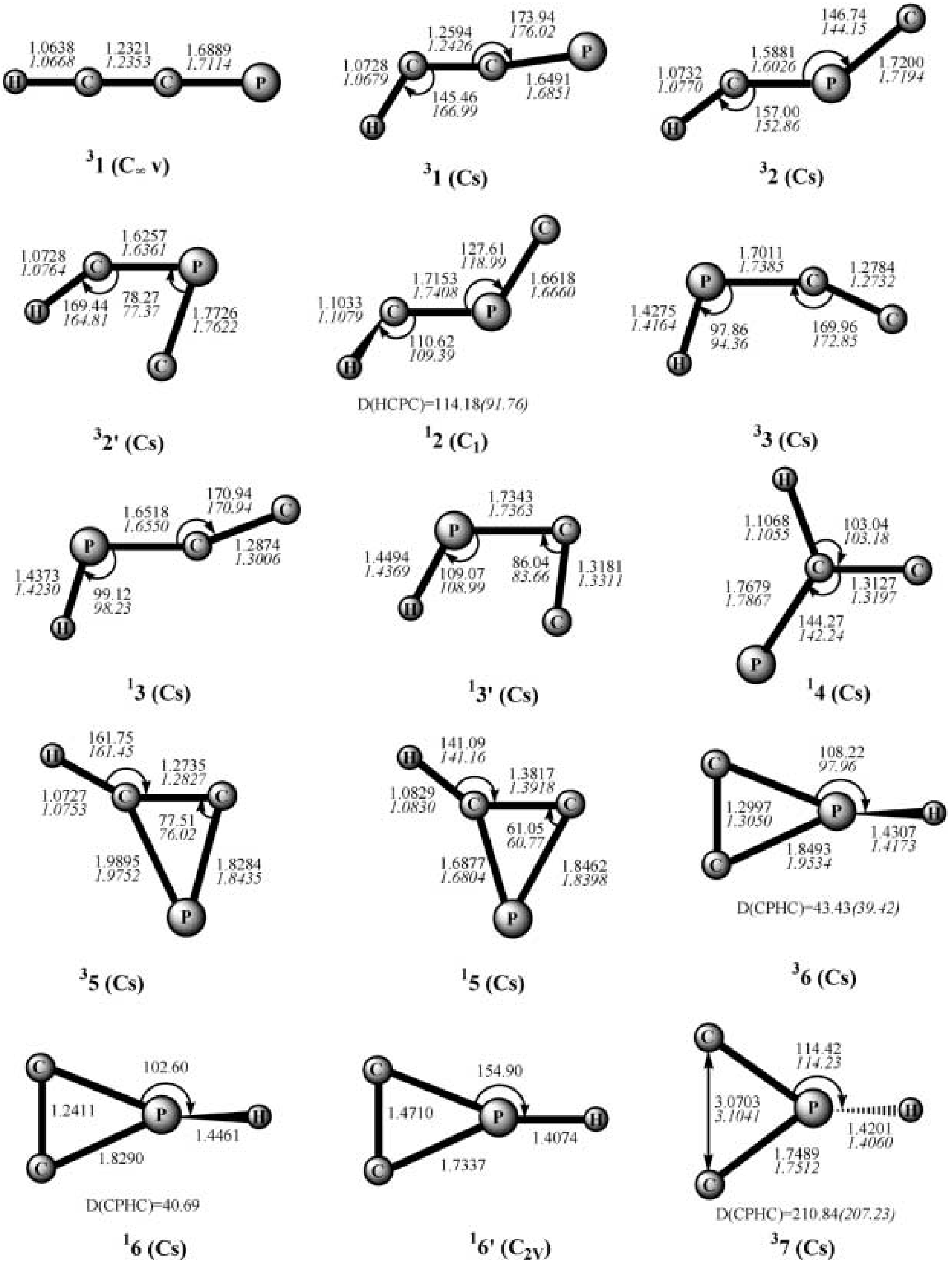

Fig. 1. Optimized geometries of HC_2P isomers at the B3LYP and QCISD (in *italics*) levels with the 6-311G(d,p) basis set. The bond lengths are in angstroms and the angles in degrees. *D*(*abcd*) denotes the dihedral angle between the *abc* and *bcd* planes

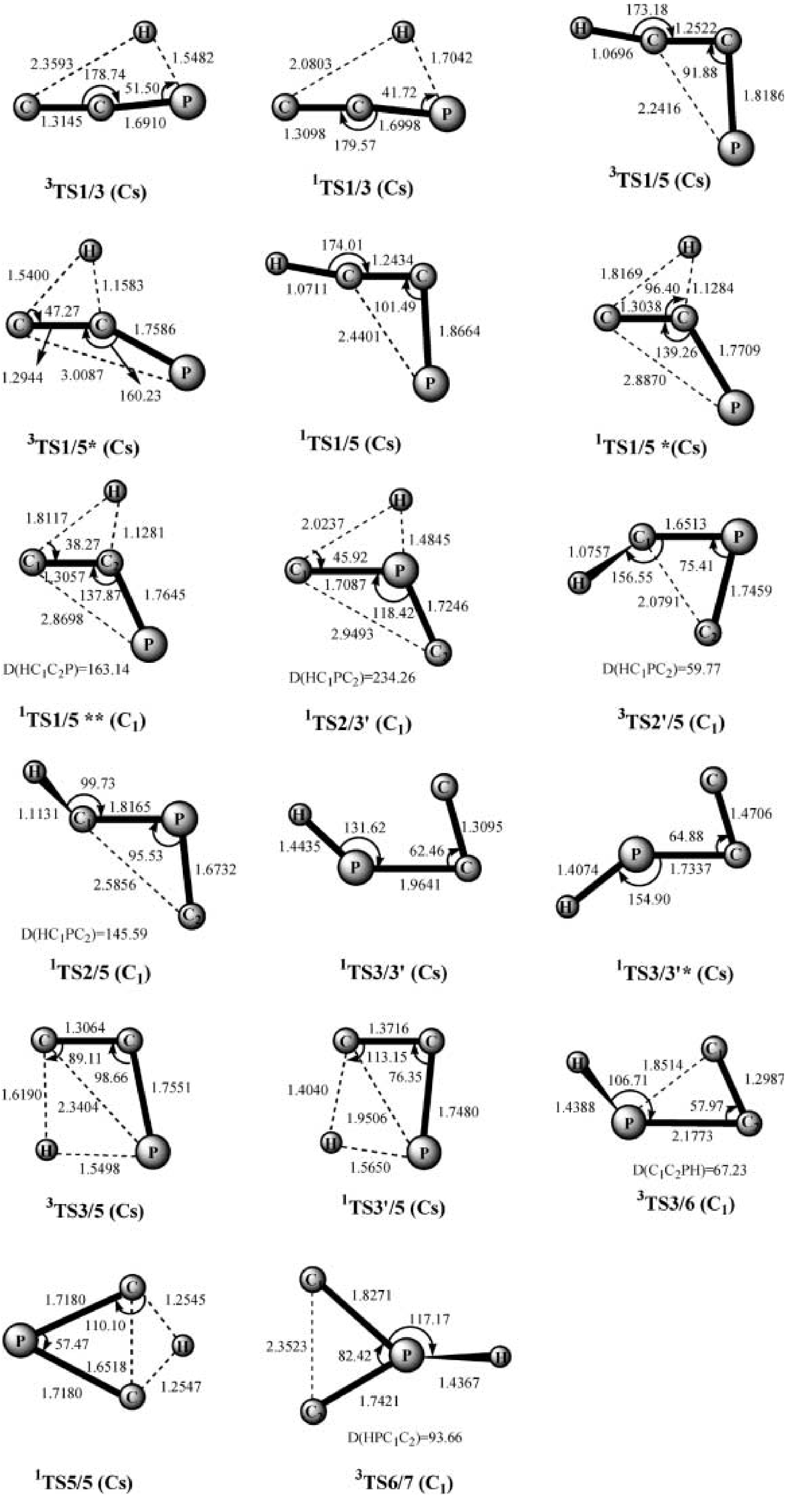

^{3}TS1/3 (Cs)

^{1}TS1/3 (Cs)

^{3}TS1/5 (Cs)

^{3}TS1/5* (Cs)

^{1}TS1/5 (Cs)

^{1}TS1/5 *(Cs)

^{1}TS1/5 ** (C$_1$)

^{1}TS2/3' (C$_1$)

^{3}TS2'/5 (C$_1$)

^{1}TS2/5 (C$_1$)

^{1}TS3/3' (Cs)

^{1}TS3/3'* (Cs)

^{3}TS3/5 (Cs)

^{1}TS3'/5 (Cs)

^{3}TS3/6 (C$_1$)

^{1}TS5/5 (Cs)

^{3}TS6/7 (C$_1$)

Fig. 2. Optimized geometries of HC$_2$P transition states at the B3LYP/6-311G(d,p) level. Bond lengths are in angstroms and angles in degrees. The symbol D(abcd) denotes the dihedral angle between the abc and bcd planes

obtained. The optimized structures of the isomers and the transition states are shown in Figs 1 and 2, respectively, while the respective vibrational frequencies of the isomers and the transition states are given in Tables 1 and 2. The energetics of all the species are listed in Table 3. Finally, a schematic PES of HC_2P in both the singlet and the triplet states is plotted in Fig. 3. Wherever possible, the similarities and discrepancies between HC_2P and HC_2N are discussed.

3.1 Triplet PES

We first consider the seven triplet isomers. The lowest-lying isomer $^{3}1$ has a linear HCCP structure in the $^{3}\sum^{-}$ state. The QCISD/6-311G(d,p) bond values are $r(CC) = 1.235$ Å, $r(CP) = 1.711$ Å and $r(CH) = 1.067$ Å. Compared with the experimentally determined structure, $r_0(CC) = 1.241$ Å, $r_0(CP) = 1.685$ Å and $r_0(CH) = 1.057$ Å [7], the agreement appears to be good.

Table 1. Harmonic vibration frequencies (cm^{-1}), IR intensities (km/mol) (in *parentheses*) and dipole moment of HC_2P isomers at the B3LYP/6-311G(d,p) and QCISD/6-311G(d,p) (in *italics*) levels

Species	Frequencies (infrared intensity)	Dipole moment (D)
^{3}1 HCCP	306 (7) 306 (7) 569 (41) 569 (41) 709 (13) 1,842 (9) 3,451 (76) *258 (4) 258 (4) 556 (40) 556 (41) 685 (25) 1,866 (17) 3,470 (58)*	1.2929 *1.0032*
^{3}2 HCPC	129 (4) 402 (46) 432 (44) 758 (28) 1,069 (28) 3,335 (42) *148 (4) 380 (39) 428 (28) 772 (26) 1,025 (32) 3,346 (33)*	3.0111 *3.1210*
^{3}2′ HCPC	269 (74) 279 (21) 485 (26) 614 (35) 1,030 (3) 3,337 (32) *175 (71) 234 (49) 433 (27) 618 (34) 1,024 (3) 3,350 (27)*	2.1021 *2.0773*
^{3}3 HPCC	269 (31) 307 (0) 674 (5) 771 (15) 1,476 (563) 2,334 (20) *252 (21) 270 (0) 671 (23) 856 (35) 1,647 (333) 2,445 (51)*	2.2861 *1.7944*
^{3}5 cCC(H)P	366 (1) 642 (41) 651 (57) 807 (40) 1,714 (11) 3,335 (40) *342 (1) 622 (50) 653 (61) 832 (43) 1,706 (11) 3,363 (36)*	1.8165 *1.8091*
^{3}6 cCP(H)C	258 (28) 388 (162) 611 (2) 769 (49) 1,585 (52) 2,286 (76) *445 (1) 470 (8) 766 (3) 873 (0) 1,597 (124) 2,421 (94)*	2.1340 *1.2285*
^{3}7 CP(H)C	119 (13) 342 (27) 720 (1) 769 (10) 791 (145) 2,349 (24) *108 (8) 321 (30) 740 (32) 783 (13) 820 (210) 2,470 (20)*	2.4629 *2.2578*
^{1}1 HCCP	241 (6) 263 (290) 403 (6) 808 (20) 1,764 (5) 3,339 (25) *231 (43) 252 (76) 372 (30) 740 (18) 1,857 (11) 3,457 (63)*	1.0900 *1.1542*
^{1}2 HCPC	118 (10) 301 (70) 662 (7) 855 (54) 1,025 (108) 3,019 (7) *151 (9) 355 (77) 691 (2) 841 (58) 1,026 (54) 3,026 (16)*	2.4839 *2.2486*
^{1}3 HPCC	155 (3) 228 (1) 799 (4) 939 (37) 1,886 (373) 2,291 (89) *132 (3) 223 (1) 797 (0) 956 (36) 1,855 (342) 2,395 (88)*	3.9635 *3.7650*
^{1}3′ HPCC	261 (2) 401 (22) 827 (3) 883 (47) 1,589 (80) 2,210 (92) *337 (1) 422 (21) 820 (0) 897 (44) 1,567 (86) 2,295 (86)*	2.6452 *2.6935*
^{1}4 CC(H)P	284 (13) 560 (49) 651 (3) 702 (28) 1,577 (44) 2,988 (67) *250 (13) 527 (40) 648 (3) 705 (16) 1,602 (64) 3,052 (44)*	2.3523 *2.2752*
^{1}5 cCC(H)P	654 (0) 813 (22) 884 (6) 1,031 (23) 1,347 (10) 3,192 (1) *675 (1) 814 (25) 910 (5) 1,066 (22) 1,345 (14) 3,252 (1)*	2.7363
^{1}6 cCP(H)C	371*i* (135) 220*i* (41) 771 (145) 975 (30) 1,943 (1) 2,228 (175)	–
^{1}6′ cCP(H)C	855*i* (88) 360 (1) 675 (6) 917 (9) 1,090 (16) 2,437 (9)	–

Table 2. Harmonic vibration frequencies (cm^{-1}) and IR intensities (km/mol) (in *parentheses*) of interconversion transition states between HC_2P isomers at the B3LYP/6-311G(d,p) level

Species	Frequencies (infrared intensity)
^{3}1/3	994*i* (8) 264 (1) 296 (12) 742 (0) 1,618 (37) 1,974 (1)
^{3}1/5	324*i* (15) 611 (60) 698 (68) 804 (25) 1,774 (7) 3,392 (68)
^{3}1/5*	166*i* (31) 346 (7) 586 (3) 662 (19) 1,690 (86) 2,617 (41)
^{3}2′/5	265*i* (44) 343 (19) 540 (34) 676 (32) 988 (8) 3,296 (19)
^{3}3/5	1,000*i* (39) 395 (0) 544 (8) 806 (1) 1,554 (54) 1,724 (25)
^{3}3/6	248*i* (34) 448 (10) 452 (71) 773 (7) 1,528 (189) 2,263 (59)
^{3}6/7	452*i* (34) 414 (53) 509 (4) 608 (20) 835 (32) 2,236 (40)
^{1}1/3	904*i* (588) 183 (4) 339 (2) 734 (7) 1,639 (126) 2,223 (52)
^{1}1/5	579*i* (112) 692 (161) 773 (38) 786 (22) 1,833 (18) 3,339 (53)
^{1}1/5*	550*i* (29) 364 (6) 616 (24) 812 (33) 1,698 (316) 2,772 (49)
^{1}1/5**	539*i* (30) 280 (11) 659 (31) 799 (23) 1,659 (171) 2,773 (27)
^{1}2/3′	1,313*i* (209) 157 (3) 550 (24) 807 (27) 899 (29) 1,958 (63)
^{1}2/5	364*i* (26) 291 (19) 643 (40) 932 (19) 1,029 (99) 2,911 (28)
^{1}3/3′	305*i* (5) 149 (1) 679 (32) 969 (9) 1,618 (33) 2,236 (89)
^{1}3/3′*	855*i* (89) 360 (1) 676 (6) 918 (8) 1,091 (16) 2,437 (9)
^{1}3′/5	927*i* (95) 725 (3) 810 (17) 822 (1) 1,342 (3) 1,887 (20)
^{1}5/5	794*i* (42) 556 (2) 872 (0) 898 (61) 1,011 (0) 2,384 (103)

Table 3. Total (a.u.) and relative (kcal/mol) (in *parentheses*) energies of the HC_2P isomers and the interconversion transition states at the B3LYP/6-311-G(d,p), QCISD/6-311G(d,p) (for isomers only) and single-point CCSD(T)/6-311G(d,p)//B3LYP/6-311G(d,p) levels

Species	B3LYP/6-311G(d,p)	CCSD(T)/6-311G(d,p)// B3LYP/6-311G(d,p)	QCISD/6-311G(d,p)
^{3}1 HCCP	−418.0899723 (0.0)	−417.3590222 (0.0)	−417.3516165 (0.0)
^{3}2 HCPC	−417.9291518 (100.9)	−417.1929670 (104.2)	−417.1907974 (100.9)
^{3}2′ HCPC	−417.9327713 (98.6)	−417.1992582 (100.3)	−417.1954259 (98.0)
^{3}3 HPCC	−417.9924004 (61.2)	−417.2563185 (64.4)	−417.2571081 (59.3)
^{3}5 cCC(H)P	−418.0343793 (34.9)	−417.3083919 (31.8)	−417.2943722 (35.9)
^{3}6 cCP(H)C	−417.9622328 (80.2)	−417.2317168 (79.9)	−417.2252945 (79.3)
^{3}7 CP(H)C	−417.8425218 (155.3)	−417.1099752 (156.3)	−417.1042357 (155.2)
^{1}1 HCCP	−418.0525094 (23.5)	−417.3257920 (20.9)	−417.3063127 (28.4)
^{1}2 HCPC	−417.9039667 (116.7)	−417.1911687 (105.3)	−417.1706243 (113.6)
^{1}3 HPCC	−418.0207675 (43.4)	−417.3019186 (35.8)	−417.2816111 (43.9)
^{1}3′ HPCC	−417.9934907 (60.5)	−417.2773461 (51.3)	−417.2548555 (60.7)
^{1}4 CC(H)P	−417.9532821 (85.8)	−417.2337104 (78.6)	−417.2162558 (84.9)
^{1}5 cCC(H)P	−418.0587611 (19.6)	−417.3423029 (10.5)	−417.3219413 (18.6)
^{1}6 cCP(H)C	−417.9755049 (71.8)		
^{1}6′ cCP(H)C	−417.9184229 (107.6)		
^{3}1/3	−417.9701458 (75.2)	−417.2386307 (75.5)	
^{3}1/5	−418.0325043 (36.1)	−417.3071759 (32.5)	
^{3}1/5*	−418.0054026 (53.1)	−417.2824222 (48.1)	
^{3}2′/5	−417.9324295 (98.9)	−417.2001050 (99.7)	
^{3}3/5	−417.9454658 (90.7)	−417.2176726 (88.7)	
^{3}3/6	−417.9541232 (85.2)	−417.2245953 (84.4)	
^{3}6/7	−417.8297445 (163.3)	−417.0956479 (165.3)	
^{1}1/3	−417.9532431 (85.8)	−417.2323577 (79.5)	
^{1}1/5	−417.9788909 (69.7)	−417.2607706 (61.7)	
^{1}1/5*	−417.9690353 (75.9)	−417.2465426 (70.6)	
^{1}1/5**	−417.9691704 (75.8)	−417.2460314 (70.9)	
^{1}2/3′	−417.7927672 (186.5)	−417.0894136 (169.2)	
^{1}2/5	−417.8964959 (121.4)	−417.1823517 (110.9)	
^{1}3/3′	−417.9865094 (64.9)	−417.2696209 (56.1)	
^{1}3/3′*	−417.9184227 (107.6)	−417.2058477 (96.1)	
^{1}3′/5	−417.9828507 (67.2)	−417.2698054 (56.0)	
^{1}5/5	−417.9755928 (71.8)	−417.2649970 (59.0)	

The results are also consistent with one recent calculation [8]. The bond length of the terminal CP is just a little longer than the typical C=P double bond, 1.673 Å, of CH_2PH [16]. Yet, both the spin density (−0.03, 0.81, −0.37, 1.60 for H, C, C, P) and the bond order (1.00, 2.61, 1.50 for HC, CC, CP bond) analyses indicate that the triplet HCCP may be best written as a resonance structure, $HC{\equiv}C{-}P \leftrightarrow H{-}C{=}C{=}P$, where the former has more weight. Then, the linear triplet HCCP has a phosphorene form slightly modified by a phosphoallene, as stated previously [8] Optimization of a possible bent structure with a phosphocarbene form often leads to the linear form ^{3}1. Note that for HC_2N, the bent HCCN form is the ground-state structure and may be described as a bent carbene with some contribution of an allene-like character.

The second low-lying triplet isomer is ^{3}5 at 31.8 kcal/mol bearing a CPC three-membered ring with a H atom linked to the carbon. The chainlike *trans*-HPCC isomer ^{3}3 and the CPC three-membered-ring isomer ^{3}6 are 64.4 and 79.9 kcal/mol, respectively, above the ^{3}1 isomer. The CPC chainlike isomers ^{3}2 (trans-), ^{3}2′ (cis-) and ^{3}7 lie much higher at 104.2, 100.3 and 156.3 kcal/mol, respectively.

The triplet PES (dashed line) in Fig. 3 clearly shows that ^{3}1 is kinetically the most stable isomer. Its smallest isomerization barrier is 32.5 kcal/mol to isomer ^{3}5. However, the rather small reverse barrier, 0.7 kcal/mol, makes the ^{3}1 → ^{3}5 conversion almost negligible. Isomer ^{3}3 possesses much smaller kinetic stability since the smallest conversion energy is 11.1 kcal/mol (^{3}3 → ^{3}1). Owing to its high energy and low kinetic stability, the observation of isomer ^{3}3 seems less likely. The experimental observation of isomers ^{3}2′, ^{3}6 and ^{3}7 is also very unlikely owing to the very small conversion barriers, i.e., –0.6 kcal/mol for ^{3}2′→ ^{3}5, 4.5 kcal/mol for ^{3}6 → ^{3}3 and 9.0 kcal/mol for ^{3}7 → ^{3}6. The transition states linking ^{3}2 cannot be located. Yet we expect that the rotation barrier from ^{3}2 to ^{3}2′ may be just a few kilocalories per mole and thus ^{3}2 may also have low kinetic stability.

On the triplet PES, similar structures of ^{3}1, ^{3}2 and ^{3}5 are also minima for HC_2N. A minor difference for structure ^{3}3 is that it is trans for HC_2P and cis for HC_2N. The *cis*-HCPC form ^{3}2′, the three-membered-ring ^{3}6 and the branched chainlike ^{3}7 were not located for HC_2N [12, 14]. Note that for structure **6**, the triplet form is stable for HC_2P, whereas the singlet is stable for HC_2N [12, 14]. The existence of ^{3}7 may be ascribed to the ability of P to participate in five-coordination. Noticeably, while the HCPC isomers ^{3}2, ^{3}2′ and ^{3}3 at 104.2, 100.3 and 64.4 kcal/mol, respectively, are not only high-lying but are also kinetically unstable towards isomerization, the corresponding HCNC structures ^{3}2 and ^{3}3 lie just 23.7 and 33.9 kcal/mol above the ground state and are kinetically very stable. The instability of HCPC may be ascribed to

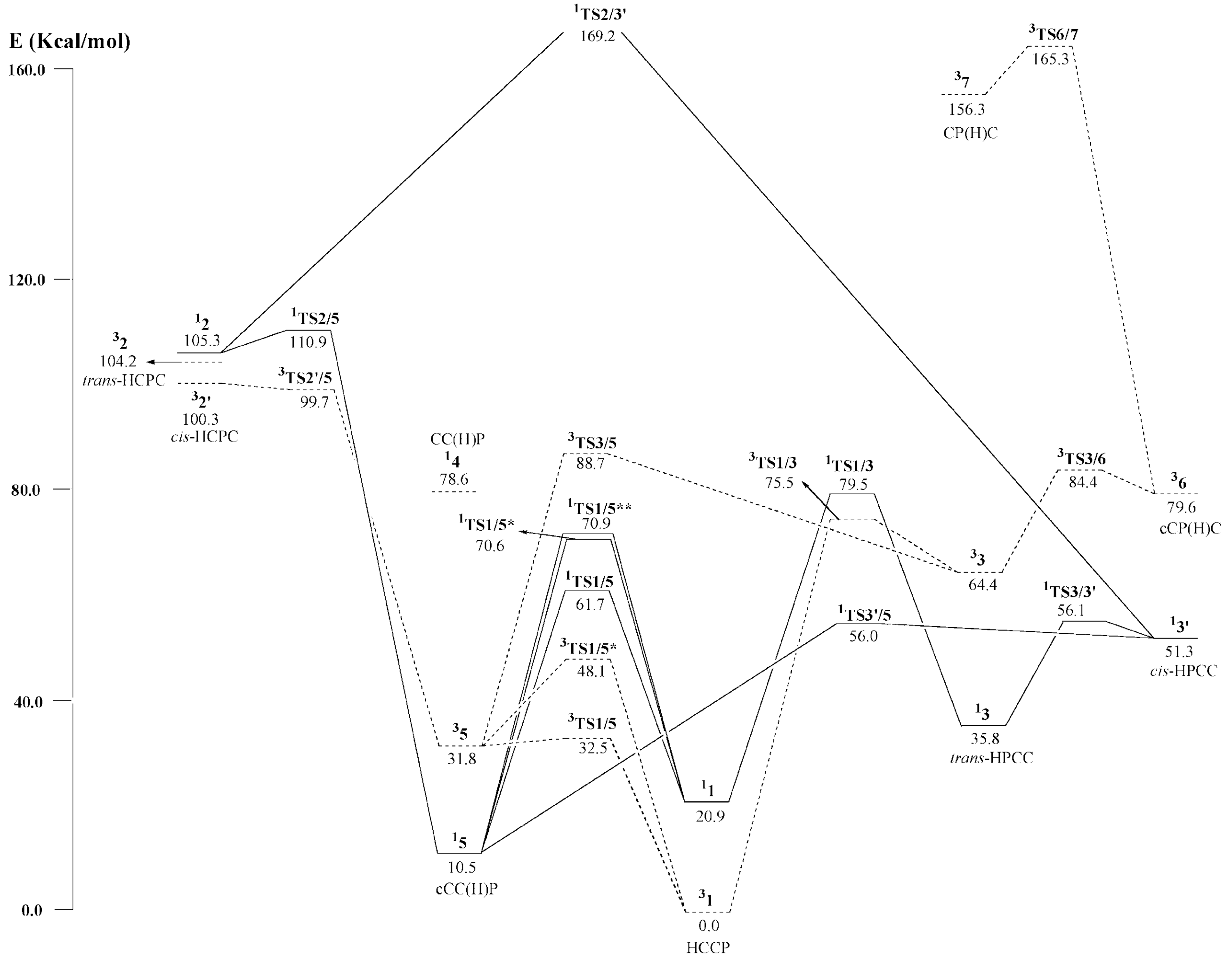

Fig. 3. Schematic potential-energy surface of HC_2P at the CCSD(T)/6-311G(d,p)//B3LYP/6-311G(d,p) level

the much lower preference of P to form multiple bonds than N.

3.2 *Singlet PES*

Let us turn to the six isomers on the singlet PES (solid line) in Fig. 3. The lowest-lying singlet isomer is the CPC three-membered-ring form $^{1}5$ (at 10.5 kcal/mol) followed by the chainlike isomers HCCP $^{1}1$ and *trans*-HPCC $^{1}3$ at 20.9 and 35.8 kcal/mol, respectively. The *cis*-HPCC $^{1}3'$ is high-lying at 51.3 kcal/mol. The branched chainlike CCP isomer $^{1}4$ with H bonded to the central C lies at 78.6 kcal/mol. Isomer HCPC $^{1}2$ is the highest singlet species, at 105.3 kcal/mol.

Considering the kinetic stability of the six singlet isomers, we can first see that $^{1}5$ is the most stable since the smallest conversion barrier is 46.5 kcal/mol ($^{1}5 \rightarrow {}^{1}3'$). The high stability of $^{1}5$ may be due to the existence of $4n + 2$ aromaticity within the three-membered ring ($n = 0$). Isomer $^{1}1$ also possesses high kinetic stability owing to the large barrier of 40.8 kcal/mol for $^{1}1 \rightarrow {}^{1}5$ conversion. The conversion barrier, 20.3 kcal/mol for $^{1}3 \rightarrow {}^{1}3'$, is much smaller than for $^{1}1$ and $^{1}5$, yet it is still considerable. Moreover, the reverse barrier from $^{1}3'$ to $^{1}3$ is just 4.8 kcal/mol, raising the kinetic stability of $^{1}3$ higher. The isomers $^{1}3'$ and $^{1}2$ may surely be considered as kinetically unstable owing to their very small conversion barriers, i.e., 5.6 kcal/mol for $^{1}2 \rightarrow {}^{1}5$ and 4.7 kcal/mol for $^{1}1 \rightarrow {}^{1}5$. We were not able to locate any transition states associated with isomer $^{1}4$ in spite of numerous attempts. Owing to the low thermodynamical stability (at 78.6 kcal/mol), we expect isomer $^{1}4$ to be of less interest.

It should be pointed out that for the well-studied HC_2N, structures similar to the *cis*-HPCC $^{1}3'$ and the branched chainlike CC(H)P $^{1}4$ do not exist. Moreover, the three-membered-ring isomers $^{1}6$ and $^{1}6'$ are not minima at all for HC_2P, whereas the corresponding HC_2N form is a minimum structure. The corresponding structure $^{1}2$ is very low lying (at 24.1 kcal/mol) and is kinetically very stable for HC_2N, whereas $^{1}2$ is rather high lying for HC_2P (at 105.3 kcal/mol) and is kinetically very unstable.

An interesting point is that for the HXCC ($X = \mathrm{N,P}$) structure, the triplet form is thermodynamically and kinetically more stable than the singlet for $X = \mathrm{N}$, while it is just the opposite for $X = \mathrm{P}$. The stability discrepancy can be reflected in the bond length variation from

Table 4. Total (a.u.) and relative (kcal/mol) (in *parentheses*) energies of the HC_2PO isomers, the transition states and fragments at the B3LYP/6-311G(d,p) and single-point CCSD(T)/6-311G(d,p) levels

Species	B3LYP/ 6-311G(d,p)	CCSD(T)/ 6-311G(d,p)// B3LYP/6-311G(d,p)
$^{1}X_{1}$ HCCPO	−493.3660927 (10.4)	−492.4829655 (13.8)
$^{1}X_{2}$ CC(H)PO	−493.3043890 (49.2)	−492.4191627 (53.8)
$^{1}X_{3}$ CCP(H)O	−493.2826797 (62.8)	−492.3964830 (68.1)
$^{1}X_{4}$ HOPCC	−493.3040561 (49.4)	−492.4172419 (55.1)
$^{1}X_{4'}$ HOPCC	−493.3096054 (45.9)	−492.4232863 (51.3)
$^{1}X_{5}$ HOCCP	−493.3173979 (41.0)	−492.4316120 (46.1)
$^{1}X_{5'}$ HOCCP	−493.3134487 (43.5)	−492.4268100 (49.1)
$^{1}X_{6}$ OC(H)CP	−493.3827236 (0.0)	−492.5050202 (0.0)
$^{1}X_{7}$ HPCCO	−493.3736111 (5.7)	−492.4845068 (12.9)
$^{1}X_{8}$ O−cCC(H)P	−493.3738688 (5.6)	−492.4881794 (10.6)
$^{1}X_{9}$ HP−cCCO	−493.2706913 (70.3)	−492.3924502 (70.6)
$^{1}X_{9'}$ HP−cCCO	−493.2703123 (70.5)	−492.3917897 (71.1)
$^{1}X_{10}$ cCC(H)PO	−493.2861719 (60.6)	−492.4061791 (62.0)
$^{1}X_{11}$ cCC(H)OP	−493.2219669 (100.9)	−492.3350866 (106.6)
$^{3}X_{1}$ HCCPO	−493.2998238 (52.0)	−492.4052433 (62.6)
$^{3}X_{2}$ CC(H)PO	−493.2304312 (95.6)	−492.3370965 (105.4)
$^{3}X_{3}$ CCP(H)O	−493.2260509 (98.3)	−492.3394041 (103.9)
$^{3}X_{4}$ HOPCC	−493.2491470 (83.8)	−492.3642728 (88.3)
$^{3}X_{4'}$ HOPCC	−493.2521263 (82.0)	−492.3673948 (86.4)
$^{3}X_{5}$ HOCCP	−493.3259007 (35.7)	−492.4358430 (43.4)
$^{3}X_{6}$ OC(H)CP	−493.2986205 (52.8)	−492.4051771 (62.7)
$^{3}X_{7}$ HPCCO	−493.3413313 (26.0)	−492.4425668 (39.2)
$^{3}X_{9}$ HP−cCCO	−493.2210533 (101.4)	−492.3351596 (106.6)
$^{3}X_{10}$ cCC(H)PO	−493.2933913 (56.1)	−492.4057912 (62.3)
$^{3}X_{11}$ cCC(H)OP	−493.2729821 (68.9)	−492.3865393 (74.3)
$^{3}X_{12}$ OCC(H)P	−493.3695521 (8.3)	−492.4810841 (15.0)
$^{3}X_{13}$ OC(H)PC	−493.2336116 (93.6)	−492.3540973 (94.7)
$^{3}X_{13'}$ OC(H)PC	−493.2275433 (97.4)	−492.3483094 (98.3)
$^{3}X_{14}$ OCPCH	−493.2971617 (53.7)	−492.4107953 (59.1)
$^{1}TSX_{1}/X_{2}$	−493.2928771 (56.4)	−492.4101260 (59.5)
$^{1}TSX_{1}/X_{3}$	−493.2053278 (111.3)	−492.3187015 (116.9)
$^{1}TSX_{1}/X_{4'}$	−493.2496346 (83.5)	−492.3645842 (88.1)
$^{1}TSX_{2}/X_{10}$	−493.2735610 (68.5)	−492.3910440 (71.5)
$^{1}TSX_{3}/X_{4}$	−493.1990030 (115.3)	−492.3097268 (122.5)
$^{1}TSX_{4}/X_{4'}$	−493.2913727 (57.3)	−492.4044951 (63.1)
$^{1}TSX_{5}/X_{5'}$	−493.2811859 (63.7)	−492.3909768 (71.6)
$^{1}TSX_{5}/X_{6}$	−493.2577140 (78.4)	−492.3729324 (82.9)
$^{1}TSX_{5'}/P_{1}$	−493.2235302 (99.9)	−492.3461407 (99.7)
$^{1}TSX_{5'}/P_{1}$*	−493.2211218 (101.4)	−492.3463816 (99.5)
$^{1}TSX_{6}/X_{8}$	−493.3078123 (47.0)	−492.4127530 (57.9)
$^{1}TSX_{6}/P_{1}$	−493.2493949 (83.7)	−492.3709771 (84.1)
$^{1}TSX_{7}/X_{8}$	−493.3006708 (51.5)	−492.4080643 (60.8)
$^{1}TSX_{7}/X_{8}$*	−493.2630311 (75.1)	−492.3796698 (78.7)
$^{1}TSX_{7}/X_{9}$	−493.2170303 (104.0)	−492.3363792 (105.8)
$^{1}TSX_{7}/P_{1}$	−493.2720523 (69.4)	−492.4017193 (64.8)
$^{1}TSX_{8}/X_{10}$	−493.2641463 (74.3)	−492.3803353 (78.2)
$^{1}TSX_{8}/P_{1}$	−493.3116002 (44.6)	−492.4295065 (47.4)
$^{1}TSX_{9}/P_{1}$	−493.2509218 (82.7)	−492.3757096 (81.1)
$^{1}TSX_{9'}/P_{1}$	−493.2433847 (87.4)	−492.3677850 (86.1)
$^{3}TSX_{1}/X_{2}$	−493.2213392 (101.3)	−492.3297406 (110.0)
$^{3}TSX_{1}/X_{3}$	−493.1886030 (121.8)	−492.2910397 (134.3)
$^{3}TSX_{1}/X_{4'}$	−493.1807574 (126.7)	−492.2878309 (136.3)
$^{3}TSX_{2}/X_{10}$	−493.2301484 (95.7)	−492.3374364 (105.2)
$^{3}TSX_{3}/X_{4}$	−493.1672720 (135.2)	−492.2771164 (143.0)
$^{3}TSX_{4}/X_{4'}$	−493.2466951 (85.4)	−492.3613982 (90.1)
$^{3}TSX_{4}/P_{11}$	−493.1511314 (145.3)	−492.2578094 (155.1)
$^{3}TSX_{5}/X_{6}$	−493.2514994 (82.3)	−492.3540414 (94.7)
$^{3}TSX_{5}/P_{3}$	−493.2599597 (77.0)	−492.3687639 (85.5)
$^{3}TSX_{6}/X_{12}$	−493.2891105 (58.7)	−492.3894236 (72.5)
$^{3}TSX_{7}/X_{9}$	−493.2145265 (105.5)	−492.3263207 (112.1)
$^{3}TSX_{7}/X_{12}$	−493.3113316 (44.8)	−492.4025650 (64.3)
$^{3}TSX_{10}/X_{12}$	−493.2814784 (63.5)	−492.3919477 (71.0)
$^{3}TSX_{12}/X_{14}$	−493.2904972 (57.9)	−492.4037502 (63.5)
$^{3}TSX_{12}/X_{14*}$	−493.2742609 (68.1)	−492.3906225 (71.8)
$^{3}TSX_{13}/X_{13'}$	−493.2264655 (98.1)	−492.3478801 (98.6)
$^{3}TSX_{13}/X_{14}$	−493.2054576 (111.1)	−492.3225469 (114.5)
R_{1} ^{3}HCCP + ^{3}O	−493.1753466 (130.1)	−492.2930193 (133.0)
R_{2} ^{1}HCCP + ^{3}O	−493.1378137 (153.7)	−492.2597891 (153.9)
R_{3} ^{3}HCCP + ^{1}O	−493.0732203 (194.2)	−492.2090401 (185.7)
R_{4} ^{1}HCCP + ^{1}O	−493.0357175 (217.7)	−412.1758099 (206.6)
R_{5} ^{1}cCC(H)P + ^{3}O	−493.1441354 (149.7)	−492.2763000 (143.5)
R_{6} ^{1}cCC(H)P + ^{1}O	−493.0420092 (213.8)	−492.1923208 (196.2)
R_{7} ^{1}HPCC + ^{3}O	−493.1061418 (173.6)	−492.2359157 (168.9)
R_{8} ^{1}HPCC + ^{1}O	−493.0040158 (237.6)	−492.1519365 (221.6)
P_{1} HCP + CO	−493.3792862 (2.2)	−492.5140872 (−5.7)
P_{2} ^{3}HCP + CO	−493.2692852 (71.2)	−492.4017643 (64.8)
P_{3} PCCO + H	−493.2691924 (71.2)	−492.3798877 (78.5)
P_{4} CCH + PO	−493.2066830 (110.5)	−492.3262155 (112.2)
P_{5} ^{3}CCO + ^{3}PH	−493.2046247 (111.8)	−492.3215600 (115.1)
P_{6} HCO + CP	−493.2150395 (105.2)	−492.3156513 (118.8)
P_{7} H + CO + CP	−493.1768383 (129.2)	−492.2927615 (133.2)
P_{8} CH + PCO	−493.1739490 (131.0)	−492.2918293 (133.8)
P_{9} HCP + ^{3}CO	−493.1620484 (138.5)	−492.2904769 (134.6)
P_{10} CCP + OH	−493.1664539 (135.7)	−492.2851225 (138.0)
P_{11} CCPO + H	−493.1556812 (142.5)	−492.2688031 (148.2)

singlet to triplet, i.e., $r(XC)$ shortens and $r(CC)$ elongates for $X = N$ [12, 14], while $r(XC)$ elongates and $r(CC)$ shortens for $X = P$. The $r(CC)$ value of HPCC is shorter than that of HNCC. At the B3LYP/6-311G(d,p) level, the bond orders are 1.81 (1.86) and 1.95 (1.87) for NC and CC bonds of singlet (triplet) HNCC, while they are 1.46 (1.36) and 2.20 (2.43) for PC and CC bonds of singlet (triplet) HPCC. This indicates that the carbene-like structure HN=C=C dominates for HNCC, whereas the acetylene-like H–P–C≡C dominates for HPCC. The atomic spin densities are 0.67, 0.16 and 1.16 for N, C and C of triplet HNCC and 0.90, 0.13 and 0.92 for P, C and C of triplet HPCC, which also supports the earlier description.

It is worth mentioning that we also carried out a comparative QCISD/6-311G(d,p) study on the structures and vibrational frequencies of minimum HC_2P isomers. As shown in Fig. 1, for nearly all the species, the B3LYP/6-311G(d,p) geometries are very close to the QCISD/6-311G(d,p) values. The exceptions are for the bond angles of the singlet HCCP $^{1}1$ and HCPC $^{1}2$, i.e., the B3LYP HCC angle is 12° smaller than the QCISD angle in $^{1}1$ and the B3LYP CPC angle and HCPC dihedral angle are about 9° and 22° larger than the QCISD values in $^{1}2$. The relatively large differences indicate that the two singlet species may have some open-shell nature.

3.3 Experimental implications

It is clear from the preceding discussions that the ground state of HC_2P is the triplet linear HCCP $^{3}1$. The second low-lying isomer is a singlet three-membered-ring $^{1}5$ at 10.5 kcal/mol. The other three forms within

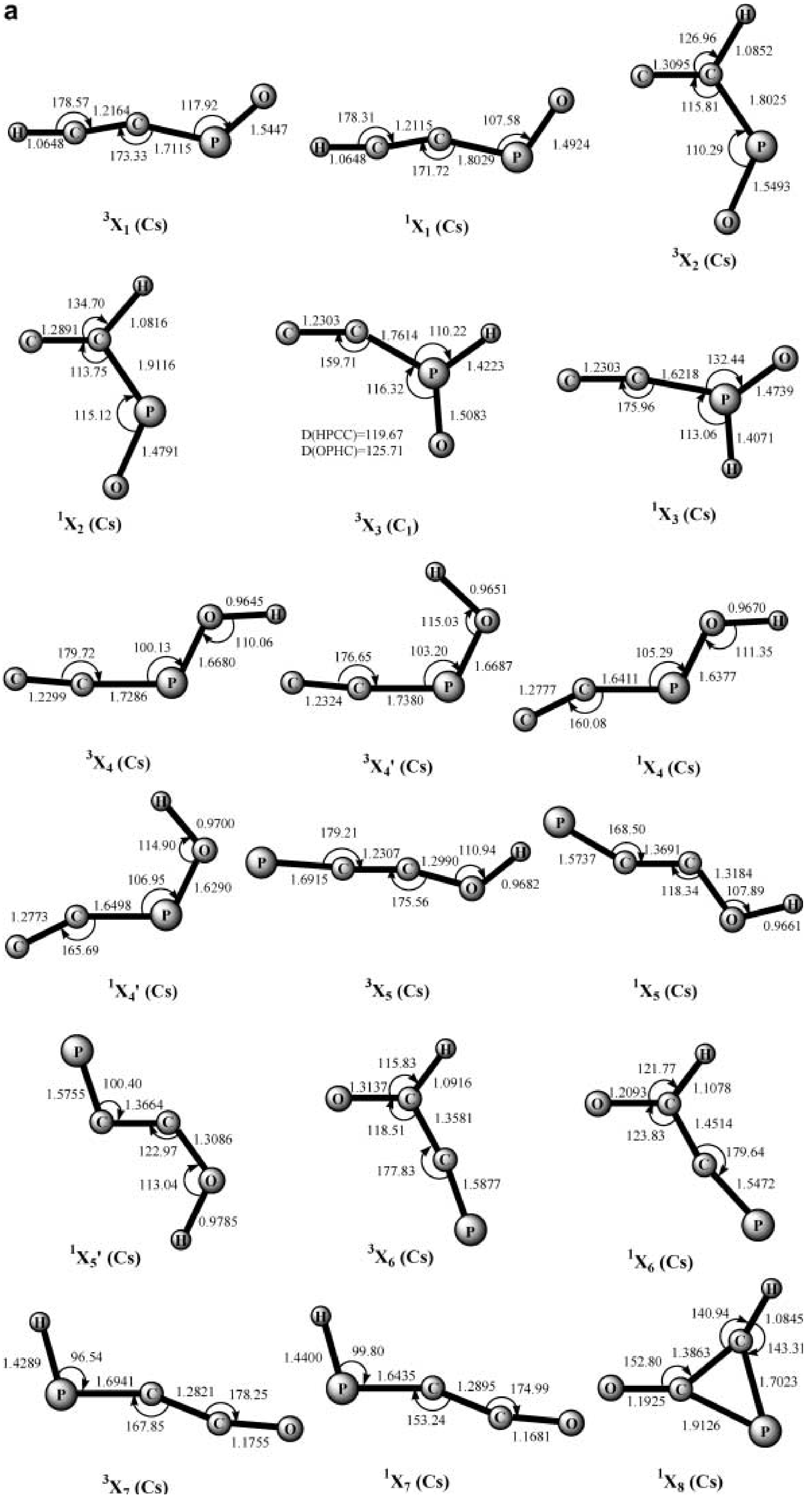

Fig. 4. Optimized geometries of HC_2PO isomers at the B3LYP/6-311G(d,p) level. Bond lengths are in angstroms and angles in degrees. The symbol D(abcd) denotes the dihedral angle between the abc and bcd planes

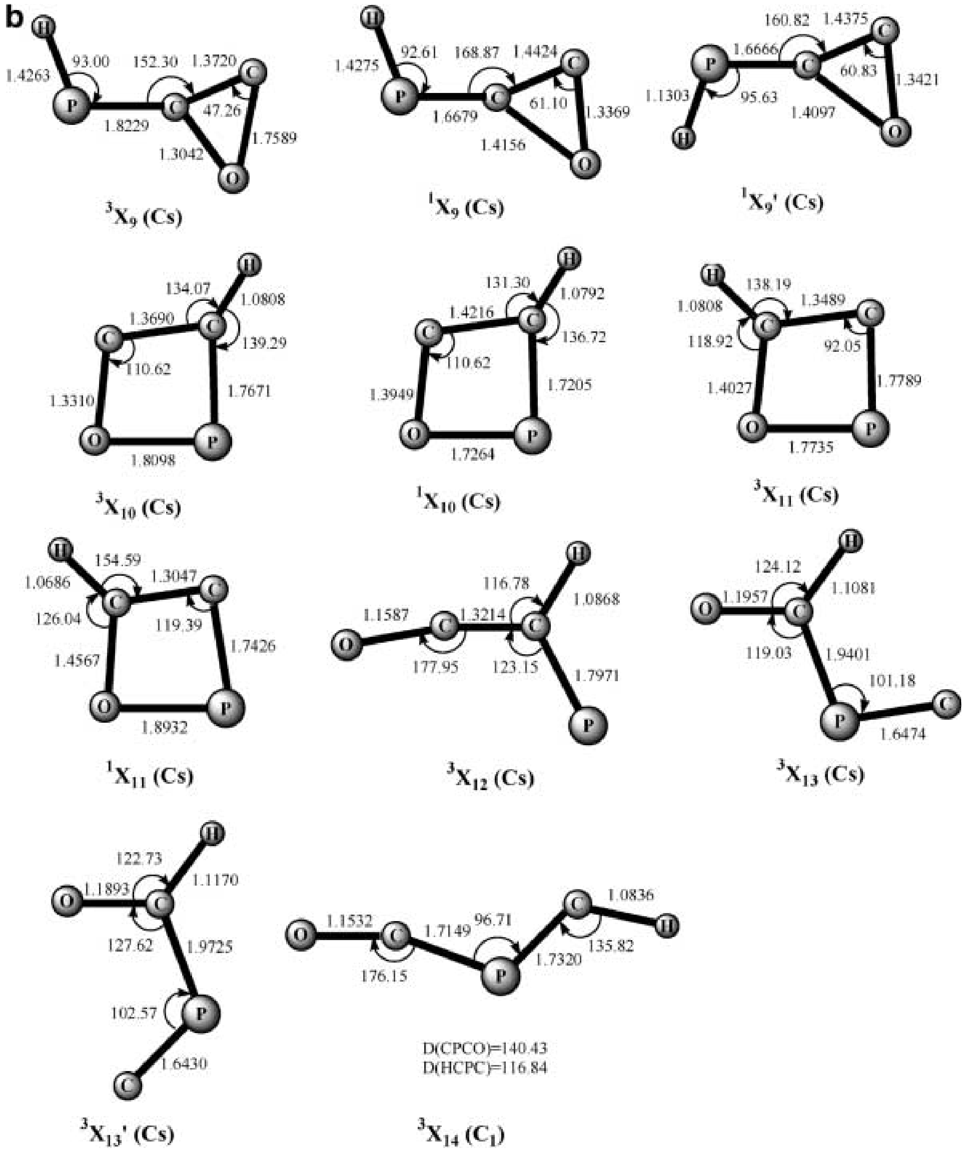

Fig. 4. (Contd.)

36 kcal/mol are ^{1}1, ^{3}5 and ^{1}3 at 20.9, 31.8 and 35.8 kcal/mol, respectively. Kinetically, only isomers ^{3}1, ^{1}1, ^{1}5 and ^{1}3 may be stable and are expected to be experimentally observable. Actually, the ground-state structure ^{3}1 has already been detected via a microwave technique [7]. Our calculations point to future interest of the singlet bent form ^{1}1. Photoexcitation of cCC(H)P **5** and HPCC **3** from singlet to triplet, however, may destabilize the structure since the corresponding triplet forms are very unstable. It has been proposed [6] that HC_2P as well as other CP-bearing molecules might be present in interstellar space if oxygen atoms are not present. On the basis of the predicted high kinetic stability, we expect the three unknown species ^{1}1, ^{1}5 and ^{1}3 to be observable under laboratory and even interstellar circumstances where oxygen atoms are very scarce. The calculated frequencies and dipole moments presented in Table 1 may be useful for future identification of ^{1}1, ^{1}5 and ^{1}3 as well as the experimentally known ^{3}1.

It is of interest to examine the reactivity of the kinetically stable HC_2P isomers HCCP ^{1}1, ^{3}1, cCC(H)P ^{1}5 and HPCC ^{1}3 towards oxygen atoms (in singlet or triplet). We performed calculations at the CCSD(T)/6-311G(d)//B3LYP/6-311G(d,p) level for both singlet and triplet PESs of the HC_2P + O reaction system (see Table 4, Figs. 4, 5, 6).[1] The evolvement of the reactions between the three HC_2P isomers and oxygen atoms can be summarized by the following pathways:

---

[1] For the HC_2P + O reaction system, the energies of the HC_2PO isomers, the transition states and fragments at the B3LYP/6-311G(d,p) and single-point CCSD(T)/6-311G(d,p) levels are listed in Table 4. The optimized geometries of the HC_2PO isomers and the transition states at the B3LYP/6-311G(d,p) level are shown in Figs. 4 and 5, respectively. A schematic PES of HC_2PO at the CCSD(T)/6-311G(d,p)//B3LYP/6-311G(d,p) level is plotted in Fig. 6

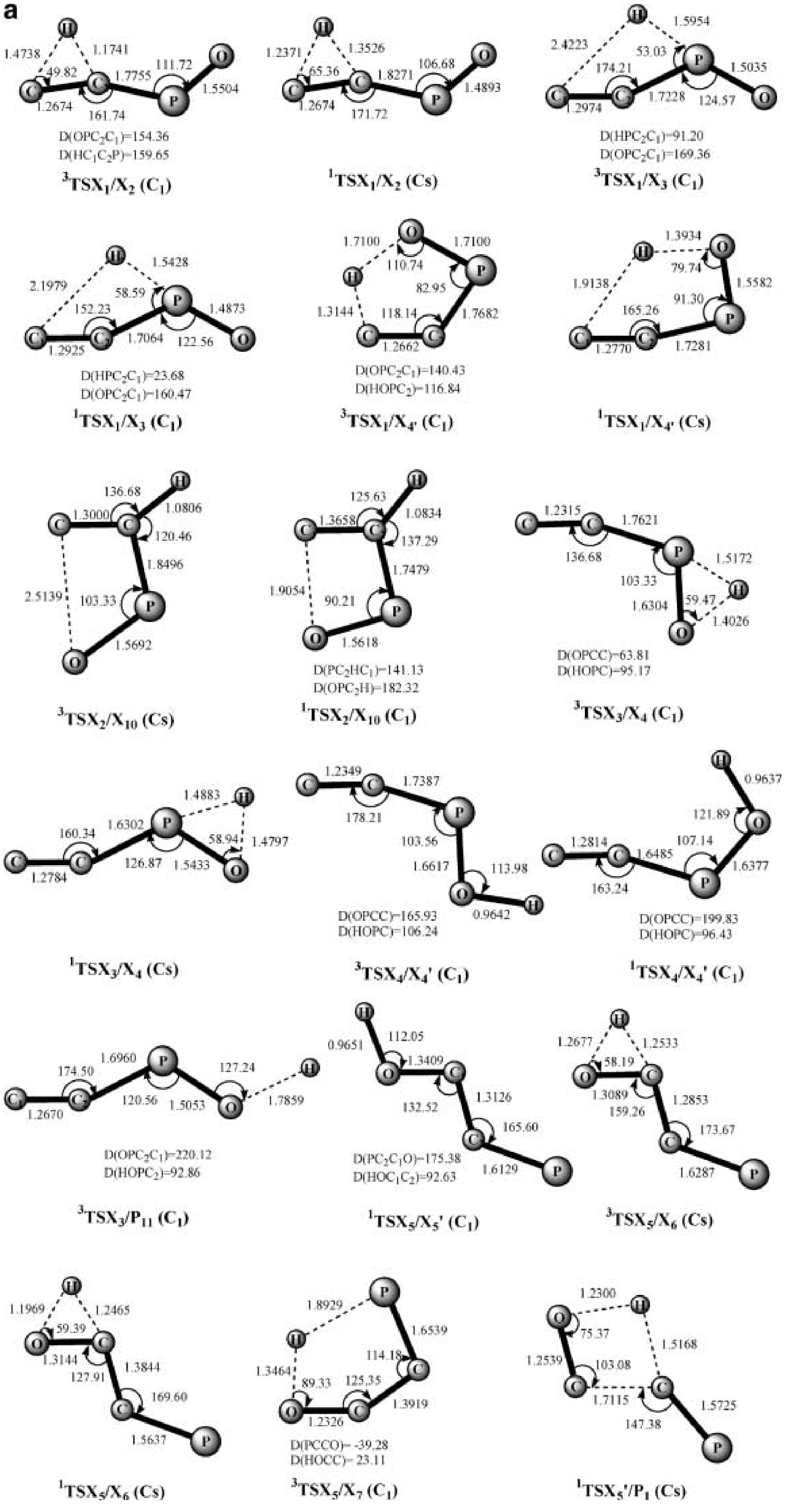

^{3}TSX$_1$/X$_2$ (C$_1$)

^{1}TSX$_1$/X$_2$ (Cs)

^{3}TSX$_1$/X$_3$ (C$_1$)

^{1}TSX$_1$/X$_3$ (C$_1$)

^{3}TSX$_1$/X$_{4'}$ (C$_1$)

^{1}TSX$_1$/X$_{4'}$ (Cs)

^{3}TSX$_2$/X$_{10}$ (Cs)

^{1}TSX$_2$/X$_{10}$ (C$_1$)

^{3}TSX$_3$/X$_4$ (C$_1$)

^{1}TSX$_3$/X$_4$ (Cs)

^{3}TSX$_4$/X$_4$' (C$_1$)

^{1}TSX$_4$/X$_4$' (C$_1$)

^{3}TSX$_3$/P$_{11}$ (C$_1$)

^{1}TSX$_5$/X$_5$' (C$_1$)

^{3}TSX$_5$/X$_6$ (Cs)

^{1}TSX$_5$/X$_6$ (Cs)

^{3}TSX$_5$/X$_7$ (C$_1$)

^{1}TSX$_5$'/P$_1$ (Cs)

Fig. 5. Optimized geometries of HC$_2$PO transition states at the B3LYP/6-311G(d,p) level. Bond lengths are in angstroms and angles in degrees. The symbol D (abcd) denotes the diheadral angle between the abc and bcd planes

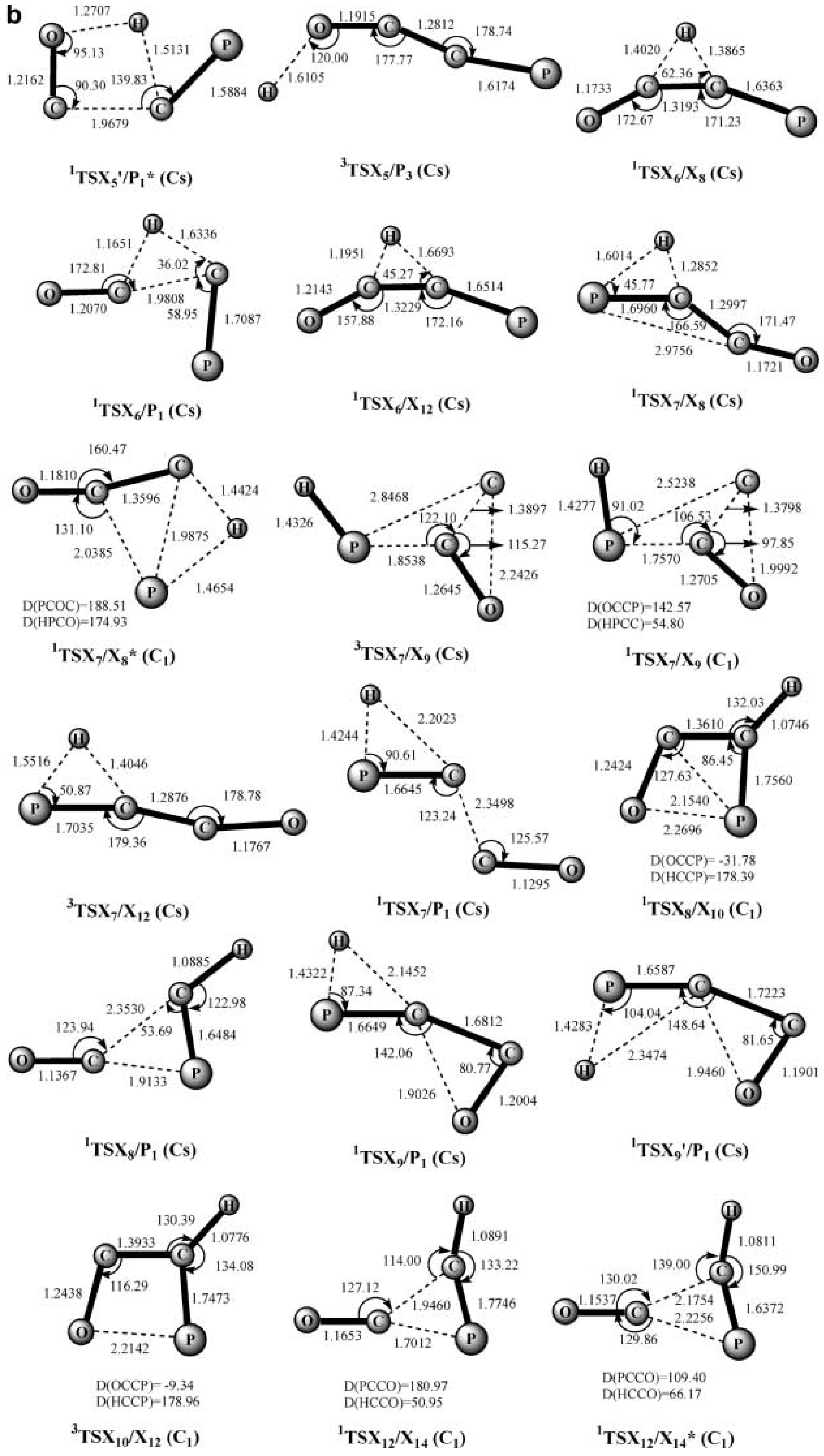

^{1}TSX$_{5}$'/P$_{1}$* (Cs)

^{3}TSX$_{5}$/P$_{3}$ (Cs)

^{1}TSX$_{6}$/X$_{8}$ (Cs)

^{1}TSX$_{6}$/P$_{1}$ (Cs)

^{1}TSX$_{6}$/X$_{12}$ (Cs)

^{1}TSX$_{7}$/X$_{8}$ (Cs)

^{1}TSX$_{7}$/X$_{8}$* (C$_{1}$)

^{3}TSX$_{7}$/X$_{9}$ (Cs)

^{1}TSX$_{7}$/X$_{9}$ (C$_{1}$)

^{3}TSX$_{7}$/X$_{12}$ (Cs)

^{1}TSX$_{7}$/P$_{1}$ (Cs)

^{1}TSX$_{8}$/X$_{10}$ (C$_{1}$)

^{1}TSX$_{8}$/P$_{1}$ (Cs)

^{1}TSX$_{9}$/P$_{1}$ (Cs)

^{1}TSX$_{9}$'/P$_{1}$ (Cs)

^{3}TSX$_{10}$/X$_{12}$ (C$_{1}$)

^{1}TSX$_{12}$/X$_{14}$ (C$_{1}$)

^{1}TSX$_{12}$/X$_{14}$* (C$_{1}$)

Fig. 5. (Contd.)

1. ^{3}HCCP or ^{1}HCCP + O → HCCPO → CC(H)PO → cCC(H)PO → O-cCC(H)P or OCC(H)P → HCP + CO (P attack).
2. ^{3}HCCP or ^{1}HCCP + O → OCHCP → O-cCC(H)P or OCC(H)P → HCP + CO (C attack).
3. ^{1}cCC(H)P + O → O–cCC(H)P or OCC(H)P → HCP + CO (C attack).
4. ^{1}HPCC + O → CCP(H)O → HCCPO → CC(H)PO → cCC(H)PO → O–cCC(H)P or OCC(H)P → HCP + CO (P attack).
5. ^{1}HPCC + O → HPCCO → O–cCC(H)P or OCC(H)P → HCP + CO (C attack).

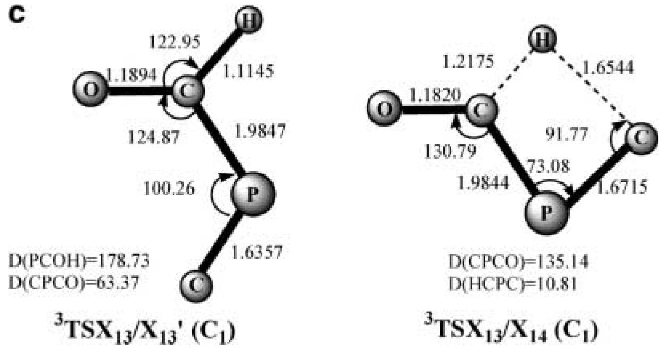

Fig. 5. (Contd.)

Note that O–cCC(H)P is in the singlet state and OCC(H)P is in the triplet state. No barriers can be found for the initial attack of these pathways. The primary products formed, HCP + CO, may undergo further dissociation to H + CO + CP except when starting from ^{3}HCCP + ^{3}O. Then, When O atoms are present (either in the singlet or in triplet state), the four inherently kinetically stable species HCCP ^{1}1, ^{3}1, H-cCPC ^{1}5 and HPCC ^{1}3 may rapidly form various HC$_2$PO intermediate isomers that may eventually dissociate to the simple fragments HCP, CP, CO and H. Formation of the other products is thermodynamically or kinetically much less competitive.

4 Conclusions

B3LYP/6-311G(d,p) and CCSD(T)/6-311G(d,p) (single-point) methods were employed to study the PES of HC$_2$P. The structural and stability properties of HC$_2$P isomers were compared with those of the well-known HC$_2$N. In addition to the experimentally known linear isomer HCCP with the $^3\sum^-$ state ^{3}1, its bent singlet form HCCP ^{1}1, the singlet three-membered-ring cCC(H)P ^{1}5 and the singlet HPCC ^{1}3 are also predicted to have considerable kinetic stability and they may be experimentally observable. However, the HCPC isomers in

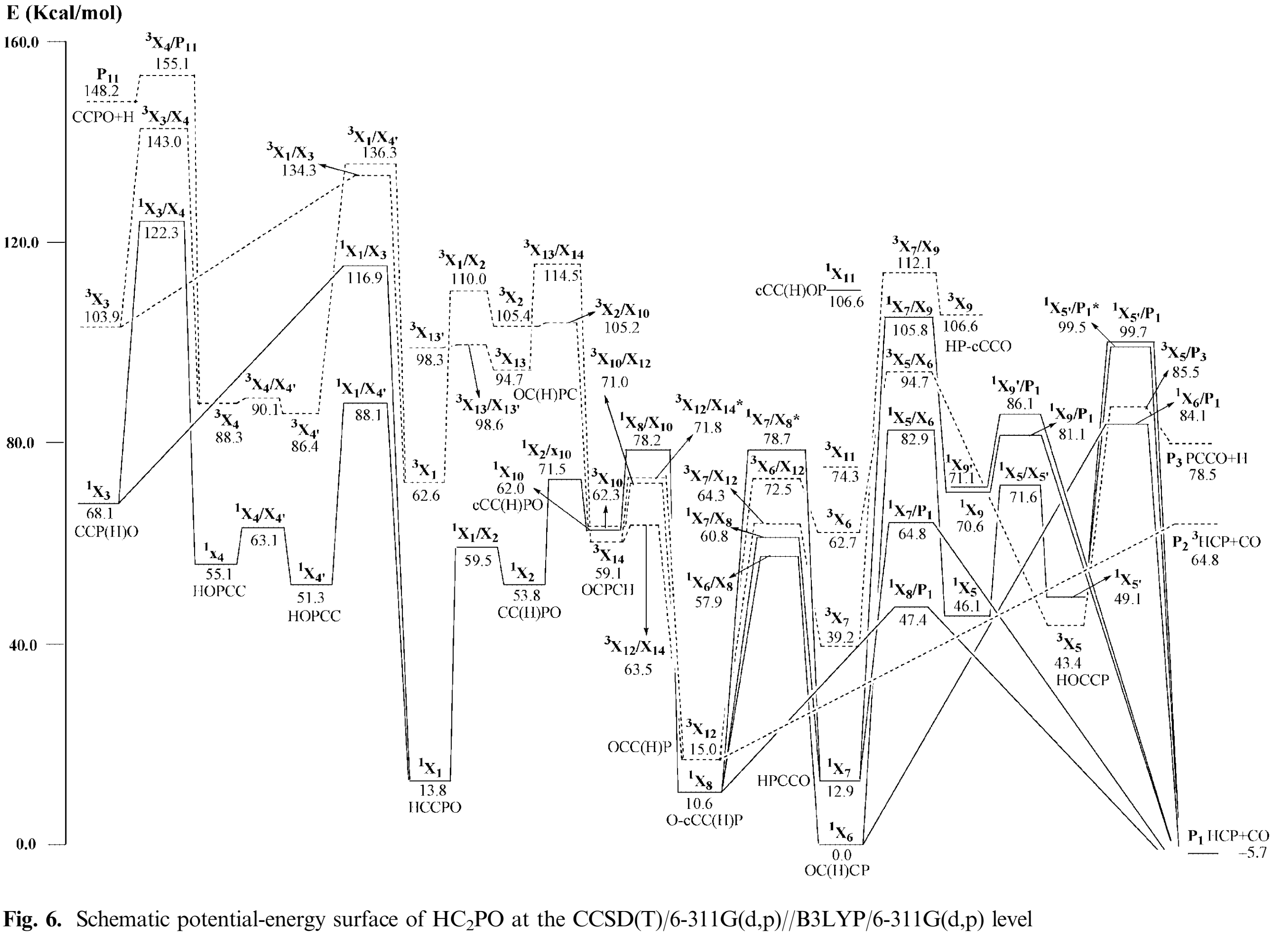

Fig. 6. Schematic potential-energy surface of HC$_2$PO at the CCSD(T)/6-311G(d,p)//B3LYP/6-311G(d,p) level

both the singlet ^{12} and the triplet ^{31} and the triplet HPCC ^{33} are energetically high lying and kinetically unstable despite the fact that the analogous triplet HCNC and HNCC are stable and have been identified experimentally. The reactivity of the species ^{11}, ^{31}, ^{15} and ^{13} towards oxygen atoms was briefly discussed. We hope that the present calculations may stimulate future characterization of these stable HC_2P isomers either in the laboratory or in interstellar space.

Acknowledgements. This work was supported by the National Natural Science Foundation of China (no. 29892168, 20073014), Doctor Foundation of Educational Ministry, Foundation for University Key Teacher by the Ministry of Education and Key Term of Science and Technology by the Ministry of Education of China. The authors are greatly thankful for the referee's helpful suggestion on discussing the reactivity of HC_2P isomers towards oxygen atoms.

References

1. Ridgeway ST, Wallace L, Smith GR (1976) Astrophys J 207: 1002
2. (a) Turner BE, Balley J (1987) Astrophys J 321: L75; (b) Ziurys LM (1987) Astrophys J 321: L81
3. Guelin M, Cernicharo J, Pauber G, Turner BE (1990) Astron Astrophys 230: L9
4. (a) Thorne LR, Anicich VG, Huntress WT Jr (1983) Chem Phys Lett 98: 162; (b) Thorne LR, Anicich VG, Prasad SS, Huntress WT Jr (1984) Astrophys J 280: 139; (c) Smith D, McIntosh BJ, Adams NG (1989) J Chem Phys 90: 6213
5. (a) Maclagan RGAR (1989) Chem Phys Lett 163: 349; (b) Maclagan RGAR (1990) J Phys Chem 94: 3373; (c) Largo A, Flores JR, Barrientos C, Ugalde JM (1991) J Phys Chem 95: 170; (d) Redondo P, Largo A, Barrientos C, Ugalde JM (1991) J Phys Chem 95: 4318; (e) Largo A, Flores JR, Barrientos C, Ugalde JM (1991) J Phys Chem 95: 6533; (f) Lopez X, Ugalde JM, Barrientos C, Largo A, Redondo P (1993) J Phys Chem 97: 1521; (g) Turner BE, Tsuji T, Balley J, Guelin M, Cernicharo J (1990) Astrophys J 365: 569
6. Millar TJ (1991) Astron Astrophys 242: 241
7. Ahmad IK, Ozeki H, Saito S (1997) J Chem Phys 107: 1301
8. Shao GQ, Fang WH (1998) Chem Phys Lett 290: 193
9. (a) Bernheim RA, Kempf RJ, Humer PW, Skell PS (1964) J Chem Phys 41: 1156; (b) Bernheim RA, Kempf RJ, Bramas JV, Skell PS (1965) J Chem Phys 43: 196; (c) Bernheim RA, Kempf RJ, Reichenbecher EF (1970) J Magn Reson 3: 5; (d) Wasserman E, Yager WA, Kuck VJ (1970) Chem Phys Lett 7: 409; (e) Bernheim RA, Bernard HW, Wang PS, Wood LS, Skell PS (1970) J Chem Phys 53: 1280; (f) Dendramis A, Leroi GE (1971) J Chem Phys 66:4334; (g) Saito S, Endo Y, Hirota E (1984) J Chem Phys 80: 1427; (h) Brown FX, Saito S, Yamamoto S (1990) J Mol Spectrosc 143: 4256
10. Flammang R, Laurent S, Flammang,-Barbieux M, Wentrup C (1993) Org Mass Spectrom 28: 1161
11. (a) Endo Y, Ohshima J (1993) Chem Phys 98: 6618; (b) Morter CL, Farhat SK, Curl RF (1993) Chem Phys Lett 207: 153; (c) McCarthy MC, Gottlieb CA, Cooksy AL, Thaddeus P (1995) J Chem Phys 103: 7779; (d) Miller CE, Eckhoff WC, Curl RF (1995) J Mol Struct 352: 435
12. Goldberg N, Fiedler A, Schwarz H (1995) J Phys Chem 99: 15327
13. (a) Hoffmann R, Zeiss GD, Van Dine GW (1968) J Am Chem Soc 90: 1485; (b) Harrison JR, Dendramis A, Leroi GE (1978) J Am Chem Soc 100: 3452; (c) Zandler ME, Goddard JD, Schaefer HF III (1979) J Am Chem Soc 101: 1072; (d) Kim KS, Schaefer HF III, Radom L, Pople JA, Binkley JS (1983) J Am Chem Soc 105: 4148; (e) Rice JE, Schaefer HF III (1987) J Chem Phys 86: 7051; (f) Malmquist P-A, Lindhm R, Roos BO, Ross S (1988) Theor Chim Acta 73: 155; (g) Seidi ET, Schaefer HF III (1992) J Chem Phys 96: 4449
14. Aoki K, Fueno H, Ikuta S, Nomura O (1993) Chem Phys Lett 202: 33
15. Winnewisser G (1997) J Mol Struct 408/409
16. Kroto HW, Nixon JF, Ohno K (1981) J Mol Spectrosc 90: 367